MECSOL 2022 - Proceedings of the 8th International Symposium on Solid Mechanics
M.L. Bittencourt, J. Labaki, L.C.M. Vieira Jr. and E. Mesquita (Editors), Campinas SP, Brazil, October 17th to 19th, 2022

Application of a fatigue phase-field framework to recover the fracture toughness of the WE43C-T5 magnesium alloy

Matheus Garcia do Vale[1], Julian Arnado Avila[2], Gualter Pereira[3], Waldek Wladimir Bose Filho[3], José Luiz Boldrini[1] and Marco Lúcio Bittencourt[1]

[1] University of Campinas, SP, Brazil
[2] São Paulo State University - São João da Boa Vista Campus, Brazil
[3] University of São Paulo - São Carlos Campus, Brazil

Material failure due to mechanical fatigue is of great concern in industry and motivation for research. Understanding crack resistance in cyclic and static load regimes is essential when we focus on solving more complex problems such as fatigue failure. Phase-field is one of the methodologies that have been employed recently to understand better phenomena including damage, fracture, and fatigue. This study applies a thermodynamically consistent and isothermal phase-field framework for damage and fatigue in small strain regime. Instead of treating fatigue phenomena based on fracture toughness degradation as in the conventional literature, this methodology models fatigue as a phase-field variable coupled with damage. The methodology has proven effective for one-dimensional cyclic loading cases and isotropic elastoplastic materials. Following the ASTM E399 standard, it is possible to validate the numerical results for a WE43C-T5 magnesium alloy using the plane-strain fracture toughness test.
Keywords: Phase-Field, Fracture, Fatigue

INTRODUCTION

The prediction of material failure is of great concern in industry and academia. A better understanding of fatigue phenomena and crack evolution is still a relevant subject. For over the last century, fracture due to fatigue was the mainstream in the experimental and theoretical fields as a result of the pioneering works of Paris and Erdogan (1963), Wöhler (1855) and Griffith (1921). However, with computer advances, methodologies such as phase field have become relevant and widely spread in literature; for instance, see Lemaitre (2013).

Phase field is a methodology capable of adequately describing interface problems such as solidification (Boettinger et al., 2002) and material phase transformation (Penrose and Fife, 1990). More recently, this methodology has been used for fracture involving, for instance, fatigue (Boldrini et al., 2016, Alessi, Vidoli and De Lorenzis, 2018, Haveroth et al., 2020), anisotropy (Petrini, Boldrini and Bittencourt, 2021) and hydrogen embrittlement (Martínez-Pañeda, Golahmar, and Niordson, 2018).

Most fracture publications treat fatigue as a fracture toughness degradation (Alessi, Vidoli, and De Lorenzis, 2018, Mesgarnejad, Imanian, and Karma, 2019, Grossman-Ponemon, Mesgarnejad, and Karma, 2022). Our framework introduces fatigue effects based on previous works, see Boldrini et al.(2016) and Haveroth et al.(2020), as an accumulation variable with evolution equation. Instead of degrading fracture toughness, fatigue variable increases the energy inside the damage domain. This point of view makes fatigue an independent phenomenon with its evolution equation and not defined empirically or *a priori* but obtained from the fundamental equations.

For high-cycle crack propagation, static failure occurs in stage 3 of the Paris curve. In this stage, when the stress intensity factor reaches its critical threshold, the propagation, once stable, becomes unstable. In this work, fatigue fracture modeling is necessary due to the pre-crack step where a small crack is propagated in the plane-strain fracture toughness test.

This manuscript is organized as follows. Firstly, a brief description of the phase-field formulation for damage and fatigue is presented. After that, the experimental and numerical procedures are described. Finally, results are presented and discussed and conclusions are addressed.

PHASE FIELD MODELING

Consider a body that at time t occupies the domain addressed by Ω_t with Eulerian coordinates $\mathbf{x}$ and $\mathcal{D}_t$ an arbitrary subdomain of Ω_t moving with the body. The symmetric part of the gradient tensor field of any given vector field $\mathbf{w}$ is

denoted by $\nabla^S\mathbf{w} = \text{sym}(\nabla\mathbf{w})$. In addition, $\mathbf{E} = \nabla^S\mathbf{u}$ and $\mathbf{D} = \nabla^S\mathbf{v}$ are the infinitesimal strain tensor and the rate of strain tensor fields respectively, where $\mathbf{u}$ and $\mathbf{v}$ are the displacement and velocity vector fields.

Two phase field variables are used to describe the damage and fatigue. The damage, denoted by φ, is considered a dynamic variable and its governing equation is obtained from the principle of virtual power (PVP). The fatigue phase field, denoted by $\mathcal{F}$, is considered an internal variable, and its governing equation is given by a constitutive differential equation that is determined when the entropy inequality is satisfied.

General governing equations for phase-field modeling

The balance equations of continuum mechanics are used to obtain a general and robust phase field model with thermodynamic consistency. The formulation of the framework is given according to Boldrini et al. (2016) and Haveroth et al. (2020).

The conservation of mass in the Eulerian description is given by

$$\dot{\rho} + \rho\,\text{div}(\mathbf{v}) = 0, \tag{1}$$

where ρ is the volumetric mass density.

The principle of virtual power (PVP) is applied to obtain following equilibrium equation at the macro scale:

$$\begin{cases} \rho\dot{\mathbf{v}} = \text{div}(\mathbf{T}) + \rho\mathbf{f} \text{ in } \mathcal{D}_t \\ \mathbf{T}\mathbf{n} = \mathbf{t} \text{ in } \partial\mathcal{D}_t \end{cases}, \tag{2}$$

where $\mathbf{T}$ is the Cauchy stress tensor field, $\mathbf{f}$ is the body load vector field and $\mathbf{n}$ is the vector field of normals to $\partial\mathcal{D}_t$. The PVP is also used in the microscale resulting at the following equilibrium equation:

$$\begin{cases} \text{div}(\mathbf{h}) - b + \rho a = 0 \text{ in } \mathcal{D}_t \\ \mathbf{h}\cdot\mathbf{n} = t_h \text{ in } \partial\mathcal{D}_t \end{cases}, \tag{3}$$

where $\mathbf{h}$ is the microstress vector field, $\mathbf{b}$ is the microforce scalar field, and a is an external body microforce.

The balance of energy, or the first principle of thermodynamics, is given as follows

$$\rho\dot{e} = \mathbf{T}:\mathbf{D} + b\dot{\varphi} + \mathbf{h}\cdot\nabla\dot{\varphi} - \text{div}(\mathbf{q}) + \rho r \;\; in\;\mathcal{D}_t, \tag{4}$$

where e is the specific internal energy, q is the heat flux vector field, and r is the specific heat source density.

Finally, from the second law of thermodynamics, we state the entropy inequality (Clausius-Duhem inequality) as

$$\rho\dot{\eta} \geq -\text{div}\left(\frac{\mathbf{q}}{\theta} + \mathbf{k}\right) + \rho\left(\frac{r}{\theta} + \omega\right) \;\; in\;\mathcal{D}_t, \tag{5}$$

where η is the specific entropy density, $\mathbf{k}$ is an entropy flux due to microscopic evolution, θ is the absolute temperature, r/θ is the specific entropy production, and ω is the entropy production due to microscopic evolution.

The equation for the fatigue variable, $\mathcal{F}$, is a differential constitutive relation and must be found in such a way that the entropy inequality is satisfied for any admissible process.

In order to obtain the thermodynamically consistent constitutive relations, the constitutive properties of the material are described in terms of the free-energy, ψ, and the pseudo-potential of dissipation, ψ_d^n. Using the balance of energy of Eq. 4, the entropy inequality, Eq. 5, is rewritten in terms of the specific free-energy $\psi = e - \theta\eta$ and given by the following:

$$-\rho\left(\dot{\psi} + \eta\dot{\theta}\right) + \mathbf{T} \;:\; \mathbf{D} + b\dot{\varphi} + \mathbf{h}\cdot\nabla\dot{\varphi} - \frac{1}{\theta}\mathbf{q}\cdot\nabla\theta + \theta\,\text{div}(\mathbf{k}) - \rho\omega\theta \geq 0. \tag{6}$$

The free energy potential depends of the internal variables as

$$\begin{cases} \psi = \psi(\Gamma) \\ \Gamma = (\rho, \theta, \varphi, \mathcal{F}, \nabla\rho, \nabla\theta, \nabla\varphi, \nabla\mathcal{F}, \mathbf{E}) \end{cases}. \tag{7}$$

Moreover, the terms $\mathbf{T}$, b, $\mathbf{h}$ and $\mathbf{q}$ are split in their reversible (non-dissipative) and irreversible (dissipative) parts and represented as $(\cdot)^r$ and $(\cdot)^{ir}$ respectively. Besides, $\mathbf{h}^{(ir)} \equiv 0$ and $\mathbf{q}^{(r)} \equiv 0$.

For the sake of simplicity, some manipulations of the previous equations will be omitted here and more details can be found in Boldrini et al. (2016).

Reversible terms are chosen such that, for any admissible process, there is no entropy increase. Considering irreversible and fatigue terms, and after some simplifications, we have the following equations:

$$b^{(ir)}\dot{\varphi} + \mathbf{T}^{(ir)} : \mathbf{D} - \frac{1}{\theta}\mathbf{q}^{(ir)} \geq 0, \tag{8}$$

$$-\rho\,\partial_{\mathcal{F}}\psi\,\mathbf{F} - \rho\,\partial_{\nabla\mathcal{F}}\psi\cdot\nabla\mathbf{F} + \theta\,\mathrm{div}(\mathbf{k}) \geq 0, \tag{9}$$

where

$$F = \tilde{F}\xi = \tilde{F}\left(\frac{\rho}{\theta}\partial_{\mathcal{F}}\psi - \mathrm{div}\left(\frac{\rho}{\theta}\partial_{\nabla\mathcal{F}}\psi\right)\right) \tag{10}$$

and $\tilde{F}$ is constant.

In order to satisfy inequality 8, we define the pseudo-potential of dissipation by

$$\psi_d^n = \psi_d^n(\dot{\varphi}, \mathbf{D}, \nabla\theta, \tilde{\Gamma}), \tag{11}$$

with

$$\tilde{\Gamma} = (\rho, \theta, \varphi, \mathcal{F}, \nabla\rho, \nabla\mathcal{F}, \mathbf{E}). \tag{12}$$

If $\psi_d^n(\dot{\varphi}, \mathbf{D}, \nabla\theta, \tilde{\Gamma}) \geq 0,\ \forall\ \left\{\dot{\varphi}, \mathbf{D}, \nabla\theta, \tilde{\Gamma}\right\}$, $\psi_d^n(0,0,0,\tilde{\Gamma}) \geq 0$ and ψ_d^n is continuous and convex with respect to the variables $\dot{\varphi}, \mathbf{D}$ and $\nabla\theta$, inequality 8 is satisfied.

After some manipulations, see Haveroth et al. (2020), Eq. 9 may be rewritten as

$$-F\xi \geq 0. \tag{13}$$

Similarly to the irreversible terms, a pseudo-potential of dissipation for fatigue is defined by the functional

$$\psi_d^{\mathcal{F}} = \psi_d^{\mathcal{F}}(\xi, \dot{\mathcal{E}}_0, \tilde{\Gamma}). \tag{14}$$

Collecting the previous equations and after some simplifications, the system of governing equations is expressed by

$$\begin{cases} \dot{\rho} + \rho\,\mathrm{div}(\mathbf{v}) = 0 \\ \dot{\mathbf{u}} = \mathbf{v} \\ \rho\dot{\mathbf{v}} = \mathrm{div}(\mathbf{T}) + \rho\mathbf{f} \\ \mathbf{T} = \rho\partial_{\mathbf{E}}\psi - \rho^2\partial_{\rho}\psi\mathbf{I} - \rho\,\mathrm{sym}\left(\nabla\mathcal{F}\otimes\partial_{\nabla\mathcal{F}}\psi + \nabla\varphi\otimes\partial_{\theta}\psi\right) + \partial_{\mathbf{D}}\psi_d^n \\ \partial_{\dot{\varphi}}\psi_d^n = \mathrm{div}(\theta\partial_{\nabla\theta}\psi_d^n) + \mathbf{T} : \mathbf{D} + (\rho\partial_{\varphi}\psi + \partial_{\dot{\varphi}}\psi_d^n)\dot{\varphi} + \rho\partial_{\nabla\varphi}\psi\cdot\nabla\dot{\varphi} + \rho r \\ e = \psi - \theta\partial_{\theta}\psi \\ \dot{\mathcal{F}} = -\partial_{\xi}\psi_d^{\mathcal{F}} \end{cases}. \tag{15}$$

The system of equations in Eq. 15 is very general. Changing the free-energy ψ and the pseudo-potentials ψ_d^n and $\psi_d^{\mathcal{F}}$, different thermodynamically consistent models that accounts for fracture and fatigue can be obtained for many types of materials.

Special case for damage and fatigue coupling

This section considers a particular case of an isothermal, isotropic, and linear elastic material with damage and fatigue. The volumetric free-energy density for a material subjected to damage is the sum of the elastic energy density $\mathcal{E}$ and the energy density related to damage and fatigue $\mathcal{J}$. Therefore,

$$\rho_0\psi(\theta, \varphi, \mathcal{F}, \nabla\varphi, \mathbf{E}) = \mathcal{E} + \mathcal{J}, \tag{16}$$

where a nearly-incompressible material is considered such that

$$\rho(\mathbf{x}, t) = \rho_0. \tag{17}$$

In order to introduce damage, we consider the elastic strain energy density of the damaged material in terms of undamaged state as

$$\mathcal{E} = g_e \mathcal{E}_0, \tag{18}$$

where g_e is the degradation function and $\mathcal{E}_0$ is the elastic strain energy density of the undamaged material. The degradation function may depend on several variables. In this work, we assume that

$$g_e(\varphi) = (1-\varphi)^{\kappa}, \tag{19}$$

where κ is a real constant.

Moreover, we split the elastic strain energy density, proposed by Amor, Marigo and Maurini (2009), into its volumetric and deviatoric (volume-preserving) contributions as follows

$$\mathcal{E}(\mathbf{E},\varphi) = g_e^+ \, \mathcal{E}_0^+(\mathbf{E}) + g_e^- \, \mathcal{E}_0^-(\mathbf{E}) \tag{20}$$

where

$$\mathcal{E}_0^+ = \frac{1}{2} K \langle \mathrm{tr}(\mathbf{E}^e) \rangle_+^2 + G(\mathbf{E}_{\mathrm{dev}}^e : \mathbf{E}_{\mathrm{dev}}^e) \tag{21}$$

and

$$\mathcal{E}_0^- = \frac{1}{2} K \langle \mathrm{tr}(\mathbf{E}^e) \rangle_-^2. \tag{22}$$

The operator $\langle \cdot \rangle_\pm$ is defined as $\langle \xi \rangle_\pm = (\xi \pm |\xi|)/2$.

The crack energy density $\mathcal{J}$ is the sum of the energy density associated with the transition layers and the total bulk energy density

$$\mathcal{J}(\varphi, \nabla\varphi) = G_c \left(\frac{\gamma}{2} |\nabla\varphi|^2 + \frac{\varphi^2}{2\gamma} \right) \tag{23}$$

where γ is a parameter related to the width of the fracture layers and G_c is the Griffith fracture energy parameter. Instead of using the traditional crack energy density, we introduce the fatigue effect in the bulk energy density as

$$\mathcal{J}(\varphi, \nabla\varphi, \mathcal{F}) = G_c \left(\frac{\gamma}{2} |\nabla\varphi|^2 + \frac{\varphi^2}{2\gamma} \right) - \frac{\mathcal{F}\varphi}{\gamma}. \tag{24}$$

Disregarding the damage gradient term and evaluating the minimum of the remainder expression, the attractor point φ shifts from 0 to 1 when $\mathcal{F}$ goes to G_c. We can expect the damage to grow faster when the fatigue reaches the fracture toughness.

The definition of the pseudo-potentials are needed. The non-plastic pseudo-potential of dissipation and the pseudo-potential associated with the fatigue process is assumed to be, respectively,

$$\psi_d^n(\dot{\varphi}, \nabla\theta, \tilde{\Gamma}) = \frac{1}{2} \tilde{\lambda}\left(\tilde{\Gamma}\right) |\dot{\varphi}|^2 \tag{25}$$

$$\psi_d^{\mathcal{F}}(\xi, \dot{\mathcal{E}}_0, \tilde{\Gamma}) = \frac{1}{2} \tilde{F}\left(\dot{\mathcal{E}}_0, \tilde{\Gamma}\right) |\xi|^2 \tag{26}$$

where $\tilde{\lambda}$ controls the damage change rate and $\tilde{F}$ is a non-negative function related to the fatigue change rate, see Boldrini et al. (2016).

Since $\tilde{F}$ must be positive in order to maintain the thermodynamical consistency and depends on the rate of undamaged elastic strain energy (works better for fatigue evolution instead of $||\mathbf{D}||$ as in Haveroth et al., 2020), the simplest choice is to assume a linear relation

$$\tilde{F} = \tilde{f}(\dot{\mathcal{E}}_0) = \tilde{a} \, g_{\mathcal{F}}(\varphi) |\dot{\mathcal{E}}_0| \tag{27}$$

where $\tilde{a}$ is a positive constant that controls the microcrack velocity. Moreover,

$$g_{\mathcal{F}}(\varphi) = (1-\varphi)^{10^{-6}} \tag{28}$$

is a function of damage that keeps the requirement of no evolution of fatigue if the material is fully cracked. Finally, after some manipulation of Eq. 15 with previous definitions, we have

$$\dot{\mathcal{F}} = \frac{\tilde{a}}{\theta\gamma}\varphi\, g_{\mathcal{F}}(\varphi)|\dot{\mathcal{E}}_0|. \tag{29}$$

In this case, the quasi-static process is considered for the motion equation. General equations in a thermodynamically consistent way are expressed in the following way:

$$\begin{cases} 0 = \dfrac{1}{\rho_0}\mathrm{div}\sigma - \dfrac{\gamma G_c}{\rho_0}\mathrm{div}(\nabla\varphi\otimes\nabla\varphi) + f \\ \dot{\varphi} = \dfrac{\gamma G_c}{\tilde{\lambda}}\Delta\varphi - \dfrac{1}{\tilde{\lambda}}(\partial_\varphi g_e^+\mathcal{E}_0^+ + \partial_\varphi g_e^-\mathcal{E}_0^-) - \dfrac{1}{\tilde{\lambda}\gamma}\left[G_c\varphi - \mathcal{F}\right] \\ \dot{\mathcal{F}} = \dfrac{\tilde{a}}{\gamma\theta}\varphi\, g_{\mathcal{F}}(\varphi)|\dot{\mathcal{E}}_0| \end{cases}, \tag{30}$$

with

$$\sigma = \partial_{\mathbf{E}^e}\mathcal{E}, \tag{31}$$

$$\frac{1}{\tilde{\lambda}} = \frac{\tilde{c}}{(1-\varphi+\delta)^\zeta}, \tag{32}$$

where $\tilde{c}$ is assumed to be a constant that controls the damage growth rate and δ a small constant to avoid numerical problems.

Notice that, considering the damage process rate-independent, which means $\tilde{\lambda} = 0$, and no fatigue phenomena, $\tilde{a} = 0$, the model recovers the model presented, for instance, in Ambati, Gerasimov and De Lorenzis, (2015).

FINITE ELEMENT APPROXIMATION

This section describes the finite element approximation of the given model. A semi-implicit time integration scheme is used to solve the equations, combining the classical Newton-Raphson (NR) iterative procedure. In general, the system of equations is solved using a *staggered* scheme as in Miehe, Welshinger and Hofacker (2010) for motion and damage, then the computation of the fatigue equation is done.

The domain is discretized by a finite element mesh. For each element with η nodes, the approximations are written as linear combinations of the local nodal basis function N_i as

$$u = \sum_{i=1}^{\eta} N_i u_i\ ,\ f = \sum_{i=1}^{\eta} N_i f_i\ ,\ \varphi = \sum_{i=1}^{\eta} \bar{N}_i\varphi_i\ ,\ \mathcal{F} = \sum_{i=1}^{\eta} \bar{N}_i\mathcal{F}_i, \tag{33}$$

$$\bar{N} = \begin{bmatrix} N_1 & N_2 & \dots & N_\eta \end{bmatrix}, \qquad N = \begin{bmatrix} N_1 & 0 & N_2 & 0 & \dots & N_\eta & 0 \\ 0 & N_1 & 0 & N_2 & 0 & \dots & N_\eta \end{bmatrix}. \tag{34}$$

The interpolation of the gradients is given by

$$\mathbf{E} = \sum B_i u_i\ ,\ \nabla\varphi = \sum \bar{B}_i\varphi_i, \tag{35}$$

where,

$$\bar{B} = \begin{bmatrix} N_{1,x} & N_{2,x} & \dots & N_{,x} \\ N_{1,y} & N_{2,y} & \dots & N_{,y} \end{bmatrix}, \quad B = \begin{bmatrix} N_{1,x} & 0 & N_{2,x} & 0 & \dots & 0 \\ 0 & N_{1,x} & 0 & N_{2,y} & \dots & N_{,y} \\ N_{1,y} & N_{1,y} & N_{2,y} & N_{2,x} & \dots & N_{,x} \end{bmatrix}. \tag{36}$$

EXPERIMENTAL AND NUMERICAL PROCEDURES

The linear-elastic plane-strain fracture toughness test is the main procedure to measure the resistance of an existing crack to propagate unstably and staticall as described in the E399 ASTM standard (ASTM E-399, 2017). To measure the critical stress intensity factor for mode I, K_{Ic}, initially, the standard specimen C(T), shown in Fig. 1, is subjected to cyclic load with foce control. The specimen is fixed in the test machine by pins assembled in the two holes.

Parameter R relates the maximum, F_{max}, and minimum, F_{min}, forces of the sinusoidal load (also given in ASTM E-647, 2016) as follows

$$R = \frac{F_{min}}{F_{max}}. \tag{37}$$

The low-intensity load pattern induces in the specimen a fatigue crack. After the fatigue crack propagates, the specimen is unloaded, and the crack length is adequately measured. Then, the specimen is subjected to a uniaxial traction with displacement control. All procedures are considered for room temperature and air environment.

The last test returns the load associated with the applied displacement, the crack mouth opening displacement (CMOD), and the crack length over time. With this data, K_{Ic} can be calculated from ASTM E-399 (2017) or ASTM E-647 (2016) standards using

$$K_I = \frac{P}{B\sqrt{W}} \frac{2+\alpha}{(1-\alpha)^{3/2}} \left(0.886 + 4.64\alpha - 13.32\alpha^2 + 14.72\alpha^3 - 5.6\alpha^4\right), \tag{38}$$

where K_I is the mode I stress intensity factor, P is the load applied to the specimen, B is the specimen thickness, W is the length indicated in Fig. 1 , $\alpha = a/W$, and a is the crack length. If some standard requirements are fulfilled, $K_I = K_{Ic}$.

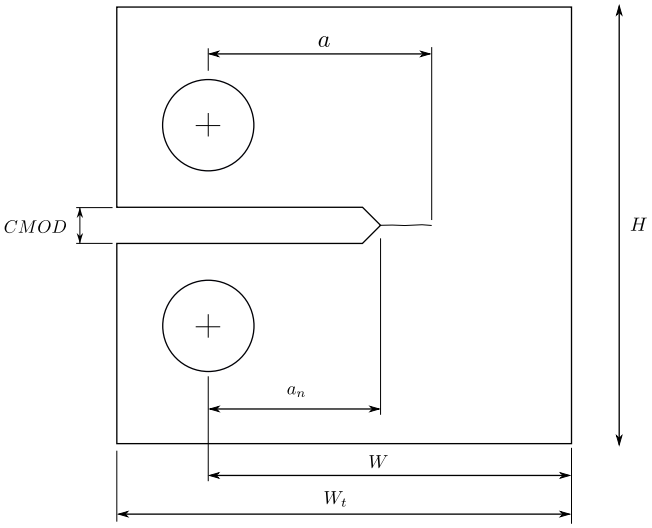

Figure 1: C(T) specimen geometry.

The motion, damage, and fatigue equation are linearized using the NR procedure for the application of the trapezoidal time integration method.

A mesh with 76000 quadrilateral linear elements is used to compute the finite element approximations. An in-house software called $(hp)^2$FEM is responsible for the computations. The numerical procedure is split into two consecutive analyses aiming to recover the experimental methods.

The first analysis comprises the fatigue phenomenon when the specimen is subjected to cyclic load. To recover the pinned condition,additional elements were added to the contact surfaces in the holes. A sinusoidal waveform load with $15Hz$ frequency is applied to both holes of the specimen, as shown in Fig. 2 with opposite directions. Moreover, boundary conditions are imposed. Two restrictions are placed on each hole center in the x-direction. Here, additional elements must be created since the nodes of the hole may rotate. To avoid rigid body motion, a displacement restriction is imposed on the center of the right edge for the y-direction.

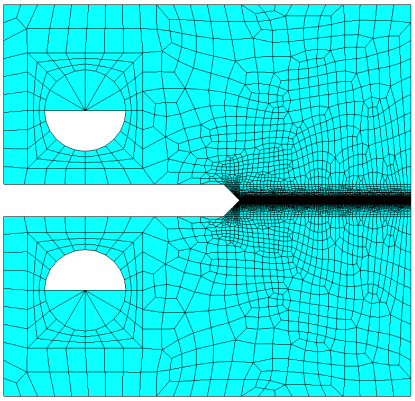

Figure 2: Finite element mesh.

In the second analysis, with the crack initiated and slightly propagated, the crack is openned. Unlike the previous analysis, this test is displacement controlled and the reaction force and the crack mouth opening displacement (CMOD) are measured. According to the standard, the force responsible for the deviation of 5% of the initial stiffness and associated to the crack length at this moment gives K_{Ic} using Eq. 38.

RESULTS

In this section, numerical results are compared with experimental data. The material considered is the WE43 magnesium alloy with material properties given in Gualter et al. (2021) and simulation parameters given in Table 1. Both experimental and numerical specimens have the same geometry with $W = 50.8\,mm$, $W_t = 63.5\,mm$, $a_n = 24.1\,mm$, hole diameters of $12.7\,mm$, thickness $B = 25.4\,mm$ and initial $CMOD = 5.0\,mm$.

Regarding cyclic analysis, time increment is given in such a way that one complete cycle is done every four time steps (located at the top, bottom, and half of the sinusoidal wave). The maximum force is $F_{max} = 5690\,N$ and the R ratio is 0.1.

In static load, the prescribed displacement is a linear function that varies with the time step number with rate of $10^{-4}\,mm/s$. The time step is $\Delta t = 1/60\,s$ and $g_e^+ = g_e^-$. $CMOD$ parameter, given in Fig. 4b, is measured as the variation of the mouth opening displacement with starting value equal to 0.

The crack length is measured in nodes where $\varphi \geq 0.999$ (see in Fig. 3 for the region in black). From Fig. 4b we obtain $P = 6700\,N$ and $a = 32\,mm$ for which $K_{Ic} \approx 18\,MPa\sqrt{m}$. Experimentally, see Fig. 4a, $K_{Ic} \approx 15\,MPa\sqrt{m}$ for $P = 8683\,[N]$ and $a = 25\,mm$.

Load and crack length values vary due to the initial crack length, which was higher for the numerical simulation. To achieve the experimental K_{Ic} with the phase field model, the most influent parameter is γ. Increasing it means that the damage field diffuses more which become more demanding for the crack to nucleate at higher φ. Besides, the final value of K_{Ic} is quite approximate.

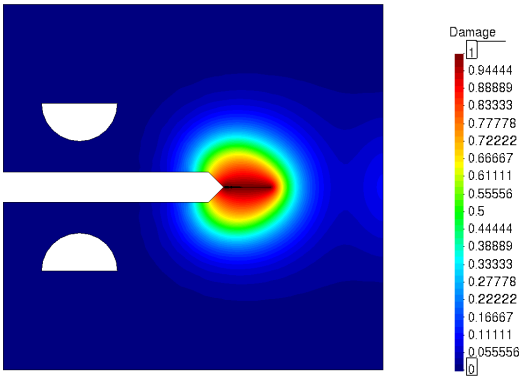

Figure 3: Damage phase field with crack (black).

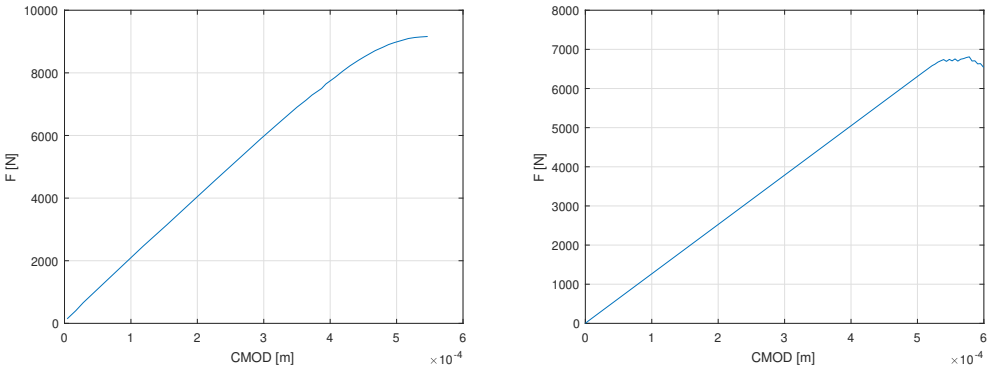

(a) (b)

Figure 4: Results for (a) experimental, and (b) numerical tests.

Table 1: Simulation parameters.

Young Modulus $[GPa]$	E	44	Poisson's Ratio	ν	0.3
Density $[kg/m^3]$	ρ_0	1830	Griffith parameter $[N/m]$	G_c	4560
Phase field parameter	ζ	1.0	Phase field parameter	$\tilde{a}$	$2.5\text{x}10^{-6}$
Phase field parameter	$\tilde{c}$	$5.0\text{x}10^{-5}$	Phase field parameter	γ	$3.5\text{x}10^{-3}$
Degradation function parameter	κ	1.5	Temperature $[K]$	θ	298.15

CONCLUSION

We have proposed a general thermodynamically consistent phase field model with a novel equation for the fatigue evolution. The fatigue equation is not assumed *a priori* as usually considered in other models but obtained from the basic equations together with the thermodynamic consistency. The choice of elastic energy rate for fatigue provides better precrack approximation and, therefore, more reliable values of K_{Ic}.

The coupled formulation of the present framework can recover cyclic (stable crack propagation) and static (unstable crack propagation) behaviors from experimental test. Moreover, the formulation is general and can be extended to other material types.

ACKNOWLEDGMENTS

The authors would like to thank the Coordenação de Aperfeiçoamento de Pessoal de Nível Superior (CAPES) for the support.

REFERENCES

Alessi, R., Vidoli, S. and De Lorenzis, L., 2018, "A phenomenological approach to fatigue with a variational phase-field model: The one-dimensional case", Engineering fracture mechanics, 190, 53-73.

Ambati, M., Gerasimov, T. and De Lorenzis, L., 2015, "Phase-field modeling of ductile fracture". Comput Mech 55, 1017–1040 (2015).

Amor, H., Marigo, J.J. and Maurini, C., 2009, "Regularized formulation of the variational brittle fracture with unilateral contact: Numerical experiments", Journal of the Mechanics and Physics of Solids, 57 (8) (2009), pp. 1209-1229.

ASTM E-399, 2017, "Standard Test Method for Linear-Elastic Plane-Strain Fracture Toughness K_{Ic} of Metallic Materials", ASTM Book of Standards.

ASTM E-647, 2016, "ASTM E647 - Standard Test Method for Measurement of Fatigue Crack Growth Rates", ASTM Book of Standards.

Boettinger, W. J., Warren, J. A., Beckermann, C. and Karma, A., 2002, "Phase-field simulation of solidification". Annual review of materials research, 32(1), 163-194.

Boldrini,J. L., Barros de Moraes,E. A., Chiarelli, L. R., Fumes, F. G. and Bittencourt, M. L., 2016, "A non-isothermal thermodynamically consistent phase field framework for structural damage and fatigue", Computer Methods in Applied Mechanics and Engineering, Volume 312, Pages 395-427.

Griffith, A. A., 1921, "The phenomena of rupture and flow in solids", Philosophical transactions of the royal society of london, Series A, 221(582-593), 163-198

Grossman-Ponemon, B. E., Mesgarnejad, A. and Karma, A., 2022, "Phase-field modeling of continuous fatigue via toughness degradation", Engineering Fracture Mechanics, 264, 108255.

Haveroth, G. A., Vale, M. G., Bittencourt, M. L. and Boldrini, J. L., 2020, "A non-isothermal thermodynamically consistent phase field model for damage, fracture and fatigue evolutions in elasto-plastic materials", Computer Methods in Applied Mechanics and Engineering, Volume 364, 112962.

Lemaitre, J. , 2013, "A Course on Damage Mechanics"

Martínez-Pañeda, E., Golahmar, A. and Niordson, C. F., 2018, "A phase field formulation for hydrogen assisted cracking", Computer Methods in Applied Mechanics and Engineering, 342, 742-761.

Mesgarnejad, A., Imanian, A. and Karma, A., 2019, "Phase-field models for fatigue crack growth", Theoretical and Applied Fracture Mechanics, 103, 102282.

Miehe, C., Welshinger, F. and Hofacker, M., 2010, "Thermodynamically consistent phase-field models of fracture: Variational principles and multi-field FE implementations", International Journal for Numerical Methods in Engineering, 83, 1273–1311.

Paris, P. C. and Erdogan, F. , 1963, "A Critical Analysis of Crack Propagation Laws", Journal of Basic Engineering, 85, 528-533.

Penrose, O. and Fife, P. C., 1990, "Thermodynamically consistent models of phase-field type for the kinetic of phase transitions", Physica D: Nonlinear Phenomena, 43(1), 44-62.

Pereira, G. S., Koga, G.Y., Avila, J. A. Bittencourt, I. M., Fernandez, F., Miyazaki, M. H., Botta, W. J. and Bose Filho, W. W., 2021, "Corrosion resistance of WE43 Mg alloy in sodium chloride solution", Materials Chemistry and Physics, Volume 272.

Petrini,A. L. E. R. ,Boldrini, J. L. and Bittencourt, M. L., 2021, "A Thermodynamically Consistent Phase Field Framework for Anisotropic Damage Propagation", Latin American Journal of Solids and Structures, 18 (1).

Wöhler, A. , 1855, "Theorie rechteckiger eiserner Brückenbalken mit Gitterwänden und mit Blechwänden", Zeitschrift für Bauwesen, 5: 121–166

RESPONSIBILITY NOTICE

The authors are the only parties responsible for the printed material included in this paper.